RSC Advances

ROYAL SOCIETY OF CHEMISTRY

www.rsc.org/advances

The use of zinc oxide nanoparticles to enhance the antibacterial properties of light-activated polydimethylsiloxane containing crystal violet

Ekrem Ozkan[a], Feyza Tunali Ozkan[a], Elaine Allan[b] and Ivan P. Parkin*[a]

[a]*Materials Chemistry Research Centre, Department of Chemistry, University College London, 20 Gordon Street, London WC1H 0AJ, UK. E-mail: i.p.parkin@ucl.ac.uk*
[b]*Division of Microbial Diseases, UCL Eastman Dental Institute, University College London, 256 Gray's Inn Road, London, WC1X 8LD, UK*

Abstract

Crystal violet-zinc oxide mixtures were incorporated into polydimethylsiloxane (PDMS) by a simple two-step method. The antibacterial activity of the polymer was tested against *Escherichia coli and Staphylococcus aureus* under white light conditions comparable to that found in a UK healthcare environment. The modified polymer demonstrated significant antibacterial activity against both bacteria (>4 log reduction in bacterial numbers). To the best of our knowledge, this is the most potent light-induced antibacterial polymer reported to date.

Introduction

Hospital-acquired infections (HAIs) cost NHS hospitals over £1 billion per annum.[1] HAIs are caused by a range of microorganisms including methicillin resistant *Staphylococcus aureus* (MRSA), *Clostridium difficile* and *Escherichia coli*. In fact, more than four million people in the EU acquire a HAI per year, of whom approximately 37,000 die because of the infection.[2]

Surfaces are potential reservoirs of bacteria correlating with the incidence of nosocomial infection.[3] Around 80 % of all nosocomial infections are thought to be transmitted through person-person contact and may not result in dangerous health complications outside a healthcare environment, however in a healthcare setting this simple transmission may lead to morbidity in patients with susceptible immune systems.[4,5] The spread of pathogens in healthcare settings may be related to inadequate hygiene regimes adopted by healthcare workers in contact with infected patients.[3,5,6] Although a rigorous hygiene regime may be advantageous, it is unlikely to completely eradicate the problem of nosocomial infection in healthcare environments where heavily contaminated surfaces are common.[3] Therefore, in order to reduce hospital contamination, new strategies need to be developed. One strategy is the utilization of bioactive surfaces that reduce transmission of infection by destroying adherent microorganisms.

There have been many investigations into self-sterilising surfaces such as TiO_2-based and copper coated materials. [7–12] In addition, the use of light-activated antimicrobial agents has emerged as a promising candidate that has arisen out of photodynamic therapy (PDT). The technique is based on using light of energy of an appropriate wavelength in combination with photosensitive dyes.[13] In this process, radical species are generated and can be regarded as non-selective microbicides[14,15] because they show a non-site specific attack mechanism against microorganisms. This strategy is unlikely to induce bacterial resistance because resistance normally develops when a microbicide targets a specific site.[14]

Photosensitive dyes such as crystal violet (CV), methylene blue (MB) and toluidine blue (TBO) have been successfully encapsulated into polymeric materials using a simple "swell-encapsulation-shrink" technique and shown to possess antibacterial activity against a wide variety of pathogenic bacteria.[16–21] The "swell-encapsulation-shrink" technique involves dipping the polymer in an organic solution of the photosensitizer which is capable of swelling the silicone polymer and allowing the photosensitizer to penetrate. After the polymer is removed from the solution, the solvent evaporates and the polymer shrinks to its original size leaving the photosensitizer incorporated in the polymer.[16,18]

Polydimethylsiloxane (PDMS) has been extensively used in a wide range of applications because of its favourable properties such as high flexibility, ease of preparation, low cost and chemical inertness.[22] Moreover, PDMS has a low glass transition temperature (T_g), high thermal and oxidative stability and good hemo- and biocompatibility.[23] These properties make it a suitable polymer host to fabricate nanocomposites.[24]

Metal nanoparticle doped polymer matrixes have attracted enormous attention due to their wide applications in optical devices,[25] microelectromechanical devices[26] and biosensors.[27,28] Much research has focused on employing a range of preparation techniques to synthesis polymer nanocomposites. Examples include: physical and chemical vapour deposition,[29] ion-implantation[30] and sol-gel process[31], in addition to the incorporation of metal nanoparticles into polymers[32,33]

Inorganic metal oxides (TiO_2, MgO, CaO and ZnO) have gained attention as antimicrobial agents because they show strong antibacterial behaviour at low concentrations.[34] Moreover, they are stable under harsh process conditions,[35,36] are normally regarded as non-toxic and some of them even include mineral elements necessary for the human body.[37,38] Among these, zinc oxide nanostructures have attracted interest because of their unique features and widespread applications. ZnO exhibits significant growth inhibition of a wide range of bacteria.[39,40] The proposed mechanism for the antibacterial behaviour of ZnO is based mainly upon catalysis of the production of reactive oxygen species (ROS) from water and oxygen,[35,41,42] that destroy the integrity of the bacterial membrane, even though additional mechanisms have also been proposed.[34,39,43–45]

The objective of this work was to study the bactericidal activity of PDMS coated with crystal violet in the presence of ZnO nanoparticles compared to the polymer containing crystal violet alone. We demonstrate a simple two-step method to prepare a potent

antimicrobial polymer-nanocomposite. The first stage involved making a homogenous mixture of zinc oxide nanopowder and PDMS followed by curing. Then, crystal violet, a photosensitizer, was incorporated into this nanocomposite using a "swell-encapsulation-shrink" process. The antibacterial activity of the modified polymers was evaluated against the Gram-negative bacterium *Escherichia coli* and the Gram-positive bacterium *Staphylococcus aureus* using a white light source comparable to those found in UK hospitals.

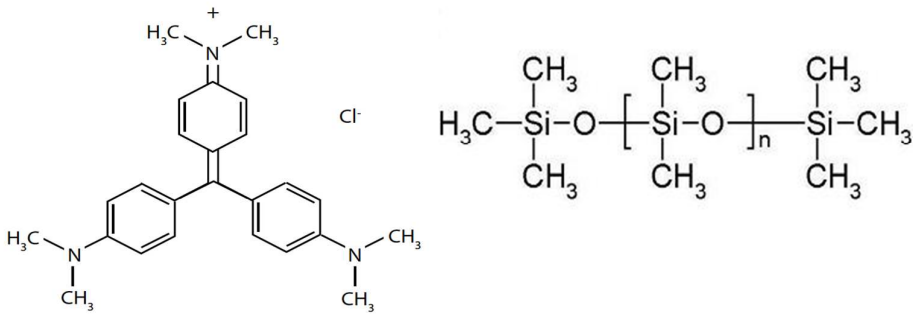

Figure 1: Chemical structures of (left) the photosensitizer dye, crystal violet, and the silicone elastomer polydimethylsiloxane[46,47]

Materials and Methods

Elastomer preparation

Blank silicone elastomers were prepared using viscous liquid Polydimethylsiloxane (Dow Corning Corporation Ltd.) as a starting material; this was mixed with the crosslinking agent in a 10:1 ratio, and spread uniformly on to a glass petri dish. The polymer was then cured at 120 °C for 60 min. After the cooling, the sheet was cut into smaller pieces (squares 1.0 x 1.0 cm).

Elastomer preparation with zinc oxide nanoparticles

4.2 g PDMS (10:1 ratio) was spread uniformly on to a glass beaker (50 cm^3). The polymer was then de-gased under vacuum until no bubbles appear (25-30 min). Afterwards, it was mixed with 0.0155 g zinc oxide nanopowder (ZnO) (< 100 nm, Sigma Aldrich and *ca*. 60 nm ± 17 measured by TEM, see ESI, Fig. S1) suspended in chloroform (3 ml). The resultant milky mixture was sonicated for 15 min to homogenise and left under vacuum for 2 days to solidify. After solidification, the resultant rigid sheet was cut into smaller pieces (squares 1.0 x 1.0 cm).

Preparation of polymers with embedded crystal violet

Crystal violet solutions (CV) were prepared at a concentration of 1000 ppm in chloroform (Sigma Aldrich). 1.0 cm^2 samples of the ZnO-containing polymer were

placed into the CV solutions and left to swell in the dark for 2 h. The samples were removed, washed and left to dry in the dark at room temperature for 24 h.

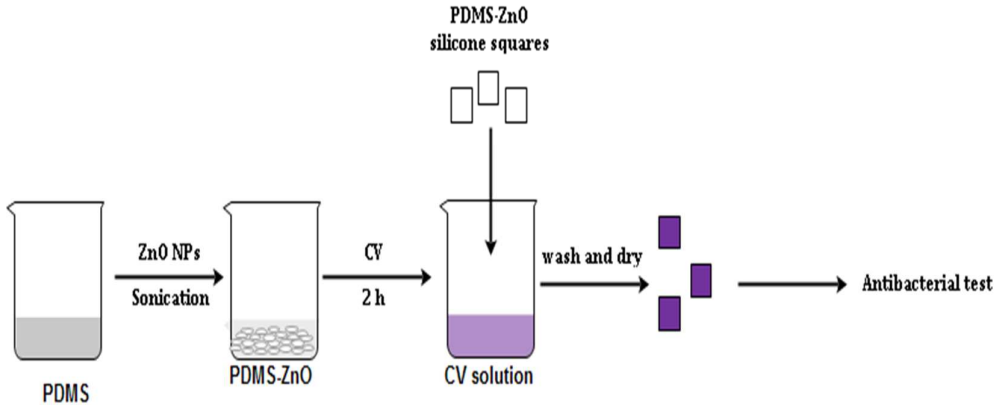

Figure 2: Schematic diagram of the synthesis procedure of derivatised PDMS polymers

Materials Characterization

A Perkin-Elmer Lambda 950 UV-vis Spectrometer was used to measure the UV-vis absorption spectra of the polymers within the range 400-800 nm. IR analysis of the polymers was performed within the range of 400-4000 cm^{-1} with an accumulation of 16 scans per sample using a Bruker Platinum ATR. Water droplet contact angles were measured using a First Ten angstroms 1000 device with a side mounted rapid fire camera fire casting 3 µL water droplet on the surface of each sample and 5 replicates on fresh samples were performed. The data was analyzed using FTA32 software. Fluoromax 4.0 Jobin Yvon Horiba spectrofluorophotometer was used to record the photoluminescence spectra of ZnO incorporated silicone at room temperature using a xenon lamp as the excitation source. The emission spectra were scanned from 350 nm to 700 nm. The excitation and emission slit width were set at 1 and 3 nm, respectively. Transmission electron microscopy (TEM) images were recorded using a JEOL JEM 1200EX with a 4 megapixel Gatan Orius SC200 charge-coupled device (CCD) camera at an acceleration voltage of 120 kV. X-ray diffraction pattern was carried out using a Stoe diffractometer with monochromated Mo Kα1 radiation (λ = 0.7093 Å) in transmission mode over the angle range 2-40°/2ϑ°.

Leaching test

The stability of the CV coated elastomers in solution was determined: crystal violet coated sections (1 cm^2) were immersed in phosphate buffered saline (PBS) (2.5 ml, 37 °C) for an extended period of time. The UV-Vis absorbance of the PBS (596 nm, Pharmacia Biotech Ultrospec 2000) was measured periodically to monitor leaching of the crystal violet from the polymer into the surrounding solution. The concentration of the CV in solution was determined on the basis of its absorbance at 596 nm, comparing it with a calibration curve.

Bactericidal assay

A range of elastomer samples (1 cm x 1 cm) was used in the antibacterial experiments: pure PDMS polymer (control), zinc oxide-incorporated (ZnO), crystal violet coated (CV),

and crystal violet and zinc oxide encapsulated silicone (CV-ZnO). These samples were evaluated against *Escherichia coli* ATCC 25922 and *Staphylococcus aureus* 8324-5. The bacteria were stored at -70 °C in Brain-Heart-Infusion broth (BHI, Oxoid) containing 20% (v/v) glycerol and propagated on either MacConkey agar (MAC, Oxoid Ltd.) in the case of *E. coli* or Mannitol Salt agar (MSA, Oxoid Ltd.) in the case of *S. aureus*, for a maximum of 2 subcultures at intervals of 2 weeks.

BHI broth (10 ml) was inoculated with 1 bacterial colony and cultured in air at 37 °C for 17 h with shaking, at 200 rpm. The bacterial pellet was recovered by centrifugation (20 °C, 4000 x g, 5 min), washed in PBS (10 ml) and centrifuged again (20 °C, 4000 x g, 5 min) to recover the bacteria, which were finally re-suspended in PBS (10 ml). The washed bacterial suspension was then diluted 1 in 1000 in PBS to give an inoculum of approximately 10^6 cfu ml^{-1}.

Duplicates of each polymer sample were inoculated with 25 µl of the inoculum and covered with a sterile cover slip (22 mm x 22 mm). The samples were then irradiated for up to ~4 hour in the case of *E. coli* and ~1 hour in the case of *S. aureus* utilizing a white light source (General Electric 28 W Watt MiserTM T5 2D compact fluorescent lamp). The light intensity was arranged to emit an average light intensity of 10500 ± 250 lux at a distance of 16 cm from the samples. A further set of samples (in duplicate) was maintained in the dark for the duration of the irradiation time. Post irradiation, the inoculated samples and cover slips were placed into PBS in a 50 ml plastic tube and vortexed for 20 seconds. The neat suspension and ten-fold serial dilutions were plated on the appropriate agar incubated aerobically overnight at 37 °C and the colonies enumerated to determine the number of surviving bacteria. The bacterial numbers in the inocula were also determined in each experiment by viable colony counting. Each experiment included two technical replicates and the experiment was reproduced three times. The data was analyzed using the Mann-Whitney U test.

Results and discussion

Synthesis

Nanoparticle embedded PDMS was prepared by dispersing zinc oxide nanoparticles using chloroform and mixing with the silicone elastomer and the crosslinking agent followed by curing. While PDMS is transparent, the zinc oxide-impregnated polymer is white. Afterwards, dye-embedded polymer was prepared with a swell-encapsulation-shrink method with 1000 ppm of CV. The polymer squares (1 cm x 1 cm) were put in a chloroform solution saturated with CV for 2 h in the dark. They were subsequently removed from the solution, washed and air-dried (24 h) so that the solvent evaporated. This method generated a purple-colored silicone that had shrunk to its original size and contained encapsulated CV (Fig. 3). Chloroform was utilized as a solvent since it not only solubilizes the dye and PDMS, but it also swells the samples to a large extent to enable CV incorporation into the polymer matrix. Furthermore, the presence of ZnO in the polymer was calculated at 0.36%.

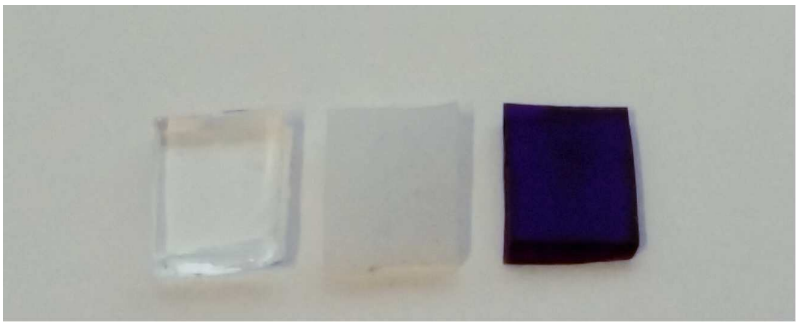

Figure 3: Images of silicone samples; bare PDMS (left), ZnO-PDMS (middle) and CV-ZnO-PDMS (right)

Characterization

The IR spectrum of the samples was obtained by ATR. The spectra (data not shown) detected no significant change across the sample range after embedding either zinc oxide nanoparticle or CV in the polymer matrix. The results showed that embedded compounds had no influence on the physical and chemical structure of the silicones. IR spectra only gave peaks related to the host polymer matrix.

The UV-vis absorbance spectra of silicone samples were measured within the range 400-800 nm (Fig. 4). While pure PDMS does not show any absorbance in the visible region, when immobilized in 100 ppm CV solution for 2 h, the main absorption peak of CV-encapsulated silicone is at $\lambda \approx 590$ nm, with a shoulder peak of weaker intensity at $\lambda \approx 533$ nm. The sample prepared with 1000 ppm crystal violet reached the saturation of the signal resulting in absorption with more intense peaks.

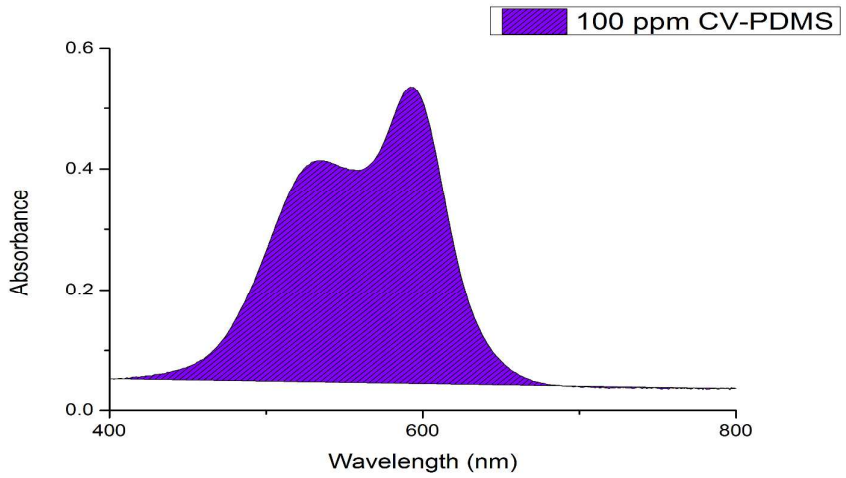

Figure 4: UV-vis absorbance spectra of CV-coated silicon polymer at a concentration of 100 ppm for 2h

Photosensitizers generate the greatest amount of ROS when illuminated at the appropriate wavelength correlated with their absorbance maximum. The light source employed in this work was a General Electric 28 W Watt MiserTM T5 2D compact fluorescent lamp with a color temperature of 3500 K, which emits light across the visible spectrum (see ESI, Fig. S2). This light source was chosen since it possesses the same characteristics as fluorescent lights utilized in hospitals in the UK. It is clear that the wavelength of the light has good overlap with CV. On the other hand, there is no emission below 410 nm wavelength and hence, the photocatalytic activity of ZnO is blocked for UV induced bacterial kill. It is well known that ZnO semiconductor possess a wide band gap of about 3.2 eV and only is able to absorb UV light wavelengths below 387 nm.[48] Hence, the bacterial kills due to light sensitivity are likely to be due only to the CV photosensitizer.

Hydrophobicity may play a crucial role in preventing bacterial adhesion. Previous studies have shown that hydrophobic surfaces were more efficient at reducing the attachment of different bacteria.[49,50] The contact angles of the polymer samples are displayed in Table 1. It is clear that the surface of bare PDMS was hydrophobic itself with a water contact angle of 106.6°. Incorporation of CV into the polymer did not cause any significant effect on the wetting property of the pure polymer while that of ZnO resulted in a more hydrophobic surface with a water contact angle greater than 120°. This might be because of the higher roughness or densely packed ZnO nanoparticles on the polymer. The CV-ZnO surface was found to be more hydrophilic compared to the ZnO polymer.

Table 1: Contact angle (°) ±SD of a range of silicone polymers: untreated (control), ZnO nanoparticle encapsulated (ZnO), crystal violet- coated (CV), crystal violet coated and zinc oxide nanoparticle encapsulated (CV-ZnO)

Samples	Water contact angle (^{0})
Control	106.6 ± 1.7
CV	109.1 ± 2.2
ZNO	120.2 ± 2.2
CV-ZnO	111.9 ± 2.2

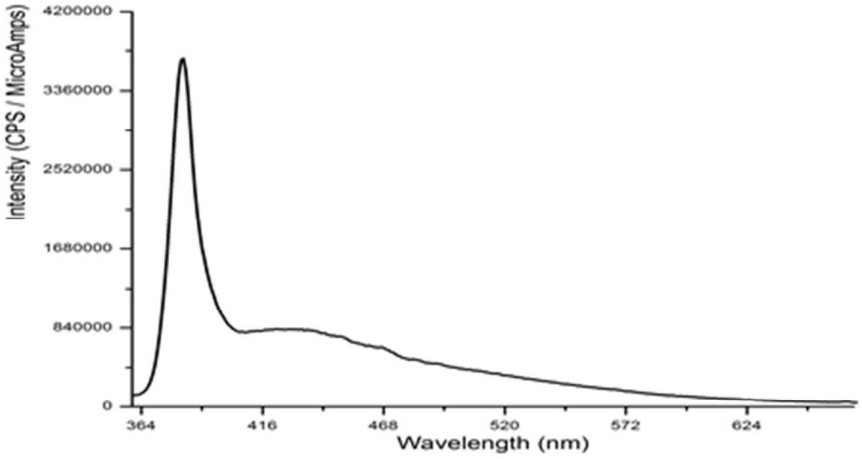

Figure 5: Room temperature PL spectra of ZnO polymer

Figure 5 depicts the photoluminescence spectra of the ZnO embedded silicone. Almost all ZnO morphologies possess two emission bands at room temperature: a near band-edge (UV) light emission (UE) and a broad, deep-level (visible) emission (VE).[51,52]The UE and VE peaks were seen at 382 and around 440 nm, respectively. The strong UE peak resulted from excitonic recombination correlated with the near band edge emission[53] while the VE peak occurred owing to defects such as oxygen vacancies that is responsible for broad-band emission.[54]

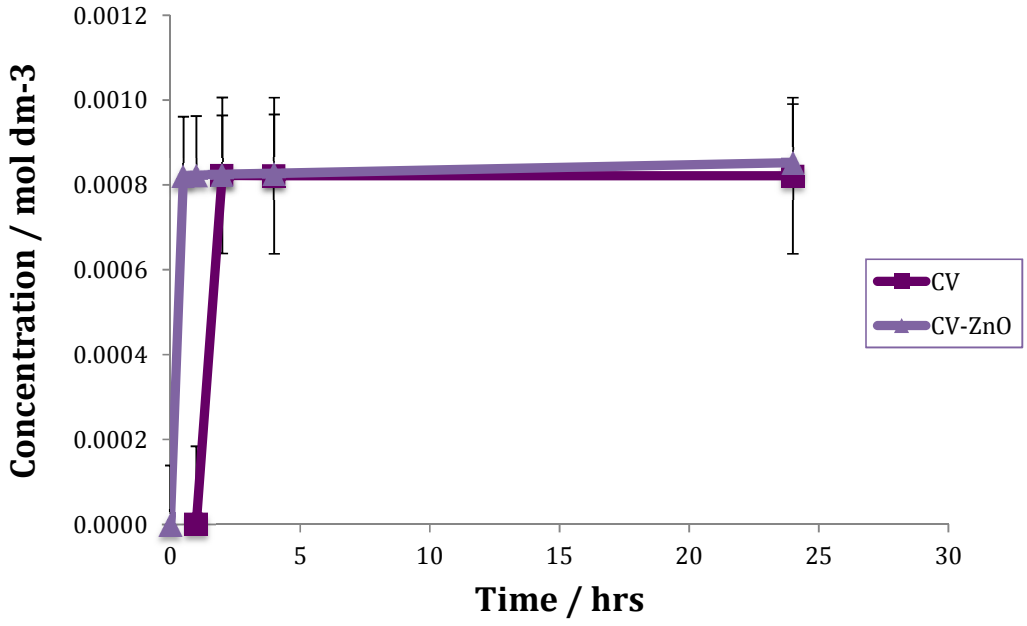

Figure 6: Leaching of crystal violet (mol dm^{-3}) from the polymers into PBS solution at 37 °C, was measured as a function of time (hours).

The leakage of CV from the CV-containing samples in aqueous solution was measured spectroscopically as a function of time (Fig. 6). The figure shows that CV-ZnO leached

some CV into the buffer upon initial immersion, whereas the polymer with only CV did not leach any dye for 1 h (the first measurement of the solutions was taken after 30 min from the samples immersion). Over a period of more than 24 h, for both samples the leaching of dye plateaued at about ≈ 0.0008 mol dm^{-3} (within experimental error). It should be noted that the leaching is due to weak surface bound CV and does not increase over time. In addition, any leaching of Zn from the polymer was not observed from either UV-vis measurements or by chemical assay indicating that ZnO is much more fixed in the polymer matrix compared to CV. In addition, the concentration of CV in the polymers was determined by UV spectroscopy using a calibration curve. The estimated CV concentration for both CV and CV-ZnO polymers were at 2 x 10^{-3} mol dm^{-3}, which demonstrates that only 2.5% of CV leached from the polymers.

Determination of the bactericidal activity of the modified polymer

The photo-induced antibacterial activity of the following samples were assessed against *S. aureus*, and *E. coli*: a control polymer sample (untreated), a zinc oxide-coated polymer sample (ZnO), a crystal violet-coated polymer sample (CV) and a crystal violet zinc oxide nanoparticle coated polymer sample (CV-ZnO). A General Electric 28 W Watt MiserTM T5 2D compact fluorescent lamp was used to activate the antibacterial activity. Also, a control set of polymers was stored under dark conditions for the duration of white light illumination.

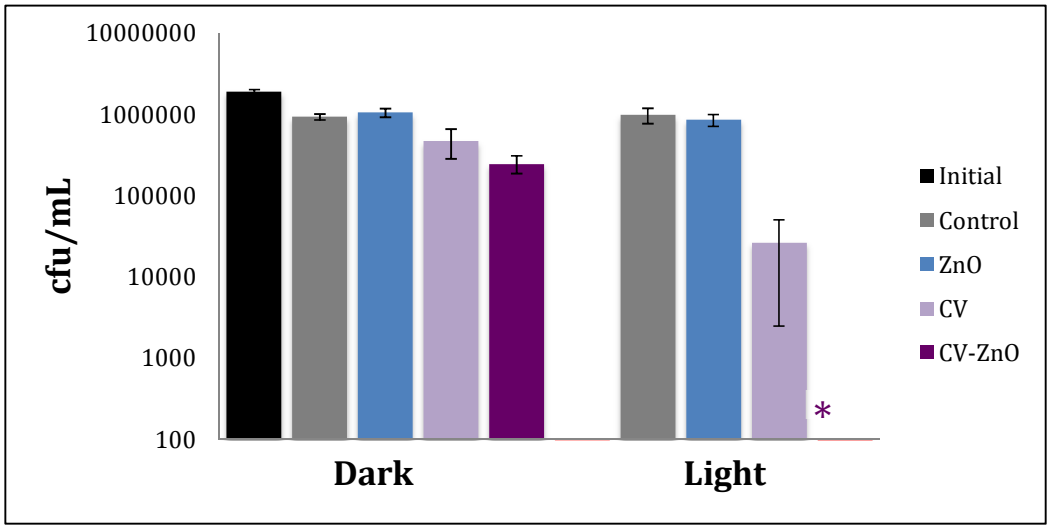

Figure 7: Numbers of *S. aureus* on the surfaces of the polymers after 1 h exposure. The asterisk indicates where the bacterial numbers are below the detection limit of 100 cfu/mL.

Fig. 7 demonstrates that under dark conditions (1 h), the ZnO encapsulated sample did not display statistically significant bactericidal activity against *S. aureus.* However, a small but statistically significant reduction in bacteria numbers compared to the control sample was achieved with all CV-coated samples ($P < 0.05$), ranging from 0.3 log kill with CV alone to a 0.5 log kill with CV-ZnO. Upon irradiation with light, neither the control nor ZnO embedded polymers showed any statistically significant kill compared

to the same samples stored under dark conditions. On the other hand, the incorporation of CV resulted in a 1.50 log reduction in the numbers of *S. aureus* compared to the ZnO sample that showed no significant activity. The effect of ZnO-CV on *S. aureus* was even more pronounced. The ZnO-CV incorporated sample showed the most potent lethal photosensitization with bacterial levels reduced below the detection limit after 1 h (>4 log reduction; P = 0.002).

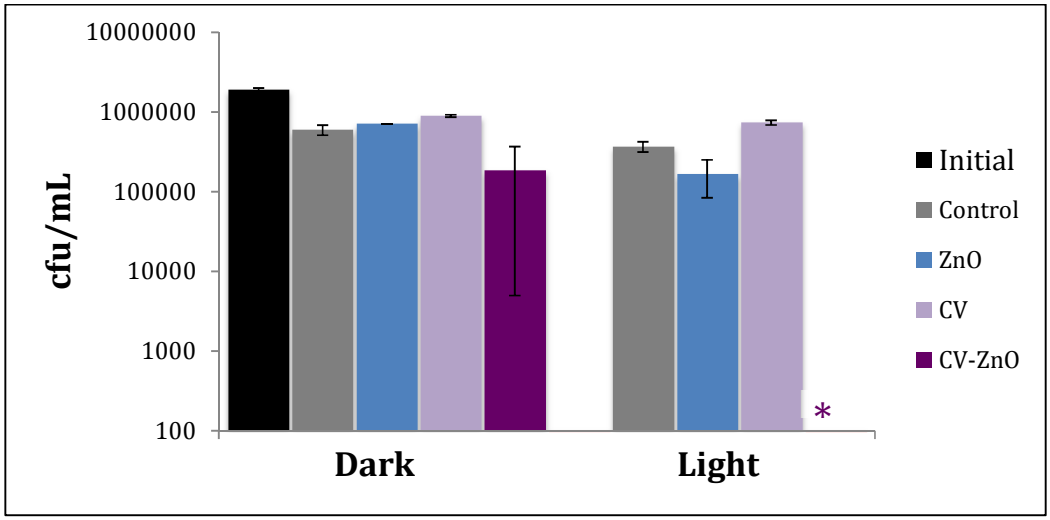

Figure 8: Numbers of *E. coli* on the surfaces of the polymers after 4 h exposure. The asterisk indicates where the bacterial numbers are below the detection limit of 100 cfu/mL.

In the case of *E. coli*, the CV and ZnO samples exhibited no statistically significant kill under dark conditions over a 4 h exposure period compared to the untreated silicone sample (Fig. 8). When zinc oxide nanoparticles and crystal violet were impregnated together, a small but statistically significant increase in bactericidal activity was observed compared to the samples containing either CV or ZnO alone ($P < 0.01$ and $P < 0.05$, respectively). Upon irradiation with white light, the polymer containing CV showed no antibacterial activity against *E. coli* while PDMS containing ZnO alone resulted in a statistically significant reduction in the number of *E. coli* ($P < 0.01$). The most significant antibacterial activity was observed with the polymer including both CV and zinc oxide NPs which showed a >4 log reduction in the numbers of *E. coli* ($P = 0.002$).

The difference in susceptibility between Gram-positive and Gram-negative bacteria can be attributed to their different cell wall structure. The cell wall of Gram-positive bacteria contains a thick layer of peptidoglycan as part of the cytoplasmic membrane whereas Gram-negative bacteria possess both inner and outer membranes.[34,55] Therefore, Gram-negative bacteria is thought to impede the uptake of photosensitizer which leads this organism to show less susceptibility against photodynamic inactivation compared to Gram-positive bacteria.

The exact mechanism of antibacterial activity of ZnO is under debate but there are several mechanisms proposed in the literature. Applerot et al. suggested the following mechanism to explain the generation of hydroxyl radicals by the reaction between water and (dissolved) oxygen over basic metals and lanthanide oxides.[42,56]

$H_2O + O_s^- \leftrightarrow \cdot OH + OH_s^-$ (1)

$2OH_s^- \leftrightarrow H_2O + \Delta + O^s{}_2^-$ (2)

$O^2 \leftrightarrow 2O_s$ (3)

$O_s + \Delta + O_s^{2-} \leftrightarrow 2O_s^-$ (4)

$O_2 + 2H_2O \leftrightarrow 4\cdot OH$ (the net reaction) (5)

Where Δ refers to an oxygen vacancy and the subscript ''s'' refers to surface species.

In addition, another possible mechanism may be the release of some Zn^{2+} from the ZnO NPs that can interact with the bacterial surface. This interaction can cause cell death as a result of the destabilization of the bacterial charge balance.[44,57,58] Another study proposed that ZnO nanoparticles attach to the outer membrane of bacterial cells generating pits in the cell wall that destroy the cell membrane. This leads to leakage of cell contents and cell death.[59]

On the other hand, unlike ZnO, the killing mechanism of CV is well established. Upon illumination, the photosensitizer dye undergoes a transition from a low energy ground state to a higher energy triplet state, where can react with biomolecules to generate free radicals (type I reaction), or with molecular oxygen to generate highly reactive singlet oxygen (type II reaction).[60] Singlet oxygen generated through type II reactions may oxidize many biological structures including proteins, nucleic acids and lipids.[61] Type I reactions result in membrane damage *via* the formation of lipid hydroperoxides and hydroxyl radicals that may react or combine with biomolecules to generate cytotoxic hydrogen peroxide *in situ*; however, the singlet oxygen produced by type II reactions generally is regarded as the major pathways in photodynamic inactivation process.[62]

Overall, we propose that ZnO nanoparticles disrupt bacterial membrane cell and increase penetration of photosensitizer into the cell, which rendered bacteria more vulnerable to photosensitization. However, to support this hypothesis, more experimental investigation should be carried out.

The crystal violet-containing samples showed stability under aqueous solutions at body temperature and therefore, transmission of the dye upon touching is improbable, reducing the possibility of subsequent adverse effects. Additionally, previous studies revealed that dye incorporated samples induce the lethal photosensitization of bacteria cells, whereas they do not cause damage to mammalian cells.[63–65] Since ROS are short lived (<1 μs)[19] with a diffusion distance of 10-100 nm in a physical environment, there is a reduced likelihood of significant long-term damage to host cells because the size of human skin cell is approximately 30 μm.[66] Notwithstanding this, more comprehensive testing of their safety *in vivo* is required before they can be used in different applications ranging from electronic devices to hospital surfaces. Regarding the colour of this new photo-activated polymer composite, key uses would be keyboards, phones, bed rails all of which a purple/black colour would be acceptable.

The intensity of the white light source used to activate the photo-antibacterial properties of the polymers including CV was 10500 ± 250 lux that can be compared with the brightness of various locations in UK hospitals, as recommended by the Department of Health.[67–69] Hence, it is anticipated that the antibacterial coating should show more efficacy in areas with higher light intensity such as examination rooms and operating theaters. Also, significant bacterial kills can be achieved in areas of lower light intensity if the illumination time is prolonged. In addition, it should be emphasised that in this study very high bacterial loads (~44 210 cfu cm^{-2} *E. coli*, ~43 973 cfu cm^{-2} *S. aureus*) were employed in order to investigate the antibacterial activity of the polymers, much higher than the level reported on contaminated hospital surfaces (up to an equivalent of 3060 cfu cm^{-2} with average values of <100 cfu cm^{-2}).[16]

Table 2: Recommended light intensities for different locations in the UK healthcare environments[68-70]

Environment	Light intensity /lx
Operating theatre	10 000-100 000
Pathology lab	8000
Ward corridors	≥ 200
A & E examination room	1000

Conclusion

In this work we have successfully embedded zinc oxide nanoparticles in PDMS followed by encapsulating CV using a ''swell-encapsulation-shrink'' method. Using standard hospital lighting conditions, the CV-ZnO polymer exhibited remarkable photobactericidal activity against *S. aureus* in just 1 h (>4 log reduction) and *E. coli* in just 4 h (>4 log reduction). Moreover, the presence of ZnO NPs improved the antibacterial activity of the polymer as well as its hydrophobicity. It is anticipated that this light-induced antibacterial dye/ ZnO nanoparticle combinations can be used in a range of applications.

Acknowledgements

The authors would like to thank to the Turkish Ministry of National Education for a scholarship to E. O. and Sacha Noimark for helpful discussions.

References

1. *Natl. Audit Off. Reducing Healthc. Assoc. Infect. Hosp. Engl.*, 2009.

2. *Health Protection Agency, English National Potint Prevalence Survey on Healthcare-associated infections and Antimicrobial use, 2011.*

3. K. Page, M. Wilson, and I. P. Parkin, *J. Mater. Chem.*, 2009, **19**, 3819.

4. P. Tierno, *Secret Life Germs, Atria Books, New York, 2001*.

5. M. Wainwright and K. B. Crossley, *Int. Biodeterior. Biodegradation*, 2004, **53**, 119–126.

6. B. Hota, *Clin. Infect. Dis.*, 2004, **39**, 1182–9.

7. C. W. Dunnill, K. Page, Z. A. Aiken, S. Noimark, G. Hyett, A. Kafizas, J. Pratten, M. Wilson, and I. P. Parkin, *J. Photochem. Photobiol. A Chem.*, 2011, **220**, 113–123.

8. K. Page, R. G. Palgrave, and I. P. Parkin, 2007, **17**, 95–104.

9. Z. A. Aiken, G. Hyett, and C. W. Dunnill, 2010, **16**.

10. C. D. Salgado, K. A. Sepkowitz, J. F. John, J. R. Cantey, H. H. Attaway, K. D. Freeman, P. A. Sharpe, H. T. Michels, and M. G. Schmidt, *Infect. Control Hosp. Epidemiol.*, 2013, **34**, 479–86.

11. P. J. McCubbin, E. Forbes, M. M. Gow, and S. D. Gorham, *J. Appl. Polym. Sci.*, 2006, **100**, 381–389.

12. D. L. Williams, K. D. Sinclair, S. Jeyapalina, and R. D. Bloebaum, *J. Biomed. Mater. Res. B. Appl. Biomater.*, 2013, **101**, 1078–89.

13. T. Dai, Y.-Y. Huang, and M. R. Hamblin, *Photodiagnosis Photodyn. Ther.*, **6**, 170–88.

14. M. Wilson, *Infect. Control Hosp. Epidemiol.*, 2003, **24**, 782–4.

15. J. C. Ireland, P. Klostermann, E. W. Rice, and R. M. Clark, *Appl. Envir. Microbiol.*, 1993, **59**, 1668–1670.

16. S. Noimark, E. Allan, and I. P. Parkin, *Chem. Sci.*, 2014, **5**, 2216.

17. S. Noimark, C. W. Dunnill, C. W. M. Kay, S. Perni, P. Prokopovich, S. Ismail, M. Wilson, and I. P. Parkin, *J. Mater. Chem.*, 2012, **22**, 15388.

18. S. Noimark, M. Bovis, A. J. MacRobert, A. Correia, E. Allan, M. Wilson, and I. P. Parkin, *RSC Adv.*, 2013, **3**, 18383.

19. S. Perni, C. Piccirillo, J. Pratten, P. Prokopovich, W. Chrzanowski, I. P. Parkin, and M. Wilson, *Biomaterials*, 2009, **30**, 89–93.

20. S. Perni, C. Piccirillo, A. Kafizas, M. Uppal, J. Pratten, M. Wilson, and I. P. Parkin, *J. Clust. Sci.*, 2010, **21**, 427–438.

21. S. Perni, P. Prokopovich, C. Piccirillo, J. Pratten, I. P. Parkin, and M. Wilson, *J. Mater. Chem.*, 2009, **19**, 2715.

22. J. N. Lee, C. Park, and G. M. Whitesides, *Anal. Chem.*, 2003, **75**, 6544–54.

23. I. Wong and C.-M. Ho, 2009, **7**, 291–306.

24. C. E. Hoppe, C. Rodriguez-Abreu, and M. Lazzari, 2008, **205**, 1455–1459.

25. Y. Dirix, C. Bastiaansen, W. Caseri, and P. Smith, *Adv. Mater.*, 1999, **11**, 223–+.

26. H. Chen, X. Liu, H. Muthuraman, J. Zou, J. Wang, Q. Dai, and Q. Huo, *Adv. Mater.*, 2006, **18**, 2876–2879.

27. M. Sulak, O. Gokdogan, and A. Gulce, 2006, **21**, 1719–1726.

28. Y. Xian, Y. Hu, and F. Liu, 2006, **21**, 1996–2000.

29. K. Giesfeldt, R. Connatser, and M. De Jesus, 2003, **57**, 1346–1352.

30. E. . Kreutz, H. Frerichs, J. Stricker, and D. . Wesner, *Nucl. Instruments Methods Phys. Res. Sect. B Beam Interact. with Mater. Atoms*, 1995, **105**, 245–249.

31. I. Yoshinaga, N. Yamada, and S. Katayama, *J. Sol-Gel Sci. Technol.*, 2005, **35**, 21–26.

32. Q. Zhang, J.-J. Xu, Y. Liu, and H.-Y. Chen, *Lab Chip*, 2008, **8**, 352–7.

33. A. Goyal, A. Kumar, P. K. Patra, S. Mahendra, S. Tabatabaei, P. J. J. Alvarez, G. John, and P. M. Ajayan, *Macromol. Rapid Commun.*, 2009, **30**, 1116–22.

34. R. Brayner, R. Ferrari-Iliou, N. Brivois, S. Djediat, M. F. Benedetti, and F. Fiévet, *Nano Lett.*, 2006, **6**, 866–70.

35. L. Zhang, Y. Jiang, Y. Ding, M. Povey, and D. York, *J. Nanoparticle Res.*, 2006, **9**, 479–489.

36. J. Sawai and T. Yoshikawa, *J. Appl. Microbiol.*, 2004, **96**, 803–9.

37. M. Roselli, A. Finamore, I. Garaguso, M. S. Britti, and E. Mengheri, *J. Nutr.*, 2003, **133**, 4077–82.

38. T. Gordon, B. Perlstein, O. Houbara, I. Felner, E. Banin, and S. Margel, *Colloids Surfaces A Physicochem. Eng. Asp.*, 2011, **374**, 1–8.

39. N. Jones, B. Ray, K. T. Ranjit, and A. C. Manna, *FEMS Microbiol. Lett.*, 2008, **279**, 71–6.

40. L. K. Adams, D. Y. Lyon, and P. J. J. Alvarez, *Water Res.*, 2006, **40**, 3527–32.

41. O. Seven, B. Dindar, S. Aydemir, D. Metin, M. . Ozinel, and S. Icli, *J. Photochem. Photobiol. A Chem.*, 2004, **165**, 103–107.

42. G. Applerot, A. Lipovsky, R. Dror, N. Perkas, Y. Nitzan, R. Lubart, and A. Gedanken, *Adv. Funct. Mater.*, 2009, **19**, 842–852.

43. Y. Liu, L. He, A. Mustapha, H. Li, Z. Q. Hu, and M. Lin, *J. Appl. Microbiol.*, 2009, **107**, 1193–201.

44. K. H. Tam, A. B. Djurišić, C. M. N. Chan, Y. Y. Xi, C. W. Tse, Y. H. Leung, W. K. Chan, F. C. C. Leung, and D. W. T. Au, *Thin Solid Films*, 2008, **516**, 6167–6174.

45. Z. Huang, X. Zheng, D. Yan, G. Yin, X. Liao, Y. Kang, Y. Yao, D. Huang, and B. Hao, *Langmuir*, 2008, **24**, 4140–4.

46. *Natl. Biochem. Corp., Cryst. Violet., http//www.nationalbiochem.com/pdf/pis/MC3886%20PS.pdf, accessed 22 May 2014*.

47. S. Seethapathy and T. Górecki, *Anal. Chim. Acta*, 2012, **750**, 48–62.

48. C. Shifu, Z. Wei, Z. Sujuan, and L. Wei, *Chem. Eng. J.*, 2009, **148**, 263–269.

49. C. R. Crick, S. Ismail, J. Pratten, and I. P. Parkin, *Thin Solid Films*, 2011, **519**, 3722–3727.

50. K. Page, M. Wilson, N. J. Mordan, W. Chrzanowski, J. Knowles, and I. P. Parkin, *J. Mater. Sci.*, 2011, **46**, 6355–6363.

51. V. A. Fonoberov and A. A. Balandin, *Appl. Phys. Lett.*, 2004, **85**, 5971.

52. J. Lim, K. Shin, H. Woo Kim, and C. Lee, *J. Lumin.*, 2004, **109**, 181–185.

53. Z. Wang, J. Gong, Y. Su, Y. Jiang, and S. Yang, *Cryst. Growth Des.*, 2010, **10**, 2455–2459.

54. N. E. Hsu, W. K. Hung, and Y. F. Chen, *J. Appl. Phys.*, 2004, **96**, 4671.

55. G. Fu, P. Vary, and C. Lin, 2005, **109**, 8889–8898.

56. K. B. Hewett, L. C. Anderson, M. P. Rosynek, and J. H. Lunsford, *J. Am. Chem. Soc.*, 1996, **118**, 6992–6997.

57. R. Brayner, R. Ferrari-Iliou, N. Brivois, S. Djediat, M. F. Benedetti, and F. Fiévet, *Nano Lett.*, 2006, **6**, 866–70.

58. S. George, S. Pokhrel, T. Xia, B. Gilbert, Z. Ji, M. Schowalter, A. Rosenauer, R. Damoiseaux, K. A. Bradley, L. Mädler, and A. E. Nel, *ACS Nano*, 2010, **4**, 15–29.

59. R. Wahab, A. Mishra, S.-I. Yun, I. H. Hwang, J. Mussarat, A. A. Al-Khedhairy, Y.-S. Kim, and H.-S. Shin, *Biomass and Bioenergy*, 2012, **39**, 227–236.

60. T. Maisch, *Lasers Med. Sci.*, 2007, **22**, 83–91.

61. M. R. Hamblin and T. Hasan, *Photochem. Photobiol. Sci.*, 2004, **3**, 436–50.

62. M. Wainwright, *Int. J. Antimicrob. Agents*, 2000, **16**, 381–94.

63. B. Zeina, J. Greenman, D. Corry, and W. M. Purcell, *Br. J. Dermatol.*, 2002, **146**, 568–573.

64. S. Noimark, C. W. Dunnill, C. W. M. Kay, S. Perni, P. Prokopovich, S. Ismail, M. Wilson, and I. P. Parkin, *J. Mater. Chem.*, 2012, **22**, 15388.

65. S. George and A. Kishen, *J. Endod.*, 2007, **33**, 599–602.

66. *Mach. Life, Second Ed.*

67. V. Decraene, J. Pratten, and M. Wilson, *Appl. Environ. Microbiol.*, 2006, **72**, 4436–9.

68. *CIBSE, Chart. Inst. Build. Serv. Eng. Light. Guid. LG2 Hosp. Healthc. Build. Chart. Inst. Build. Serv. Eng. London, United Kingdom., 1989.*

69. C. W. Dunnill, K. Page, Z. A. Aiken, S. Noimark, G. Hyett, A. Kafizas, J. Pratten, M. Wilson, and I. P. Parkin, *J. Photochem. Photobiol. A Chem.*, 2011, **220**, 113–123.